Microchimica Acta (2023) 190:80
https://doi.org/10.1007/s00604-023-05641-1

ORIGINAL PAPER

Aptasensor-based assay for dual-readout determination of aflatoxin B1 in corn and wheat via an electrostatic force–mediated FRET strategy

Jincheng Xiong[1,2] · Shuang He[1,2] · Linqian Qin[1,2] · Shuai Zhang[1,2] · Wenchong Shan[1,2] · Haiyang Jiang[1,2]

Received: 20 July 2022 / Accepted: 28 December 2022 / Published online: 2 February 2023

Abstracts

A rapid and sensitive aptasensor was established for the dual-readout determination of aflatoxin B1 (AFB1) utilizing an electrostatically mediated fluorescence resonance energy transfer (FRET) signal amplification strategy. In the presence of AFB1, the aptamer preferentially bound to AFB1, resulting in the aggregation of bare gold nanoparticles (AuNPs) induced by NaCl, accompanied by a change of AuNP solution from wine-red to purple. This color change was used for colorimetric channel analysis. Then, the positively charged quantum dots were introduced into reaction system and interacted with negatively charged AuNPs, which successfully converted the color signal into a more sensitive fluorescence signal through FRET. The fluorescence quenching efficiency decreased with increasing concentrations of AFB1, and the fluorescence of aptasensor gradually recovered. The variation of fluorescence intensity was employed for fluorometric channel analysis. Under the optimal conditions, the color and fluorescence signals exhibited excellent response to AFB1 concentration within the ranges 10–320 ng·mL^{-1} and 3–320 ng·mL^{-1}, respectively, and the limit of detection was as low as 7.32 ng·mL^{-1} and 1.48 ng·mL^{-1}, respectively. The proposed aptasensor exhibited favorable selectivity, good recovery (85.3–113.4% in spiked corn and wheat samples), stable reproducibility (RSD<13.3%), and satisfactory correlation with commercial kits (R^2=0.998). The aptasensor developed integrates advantages of modification-free, dual-readout, self-calibration, easy operation, and cost-effectiveness, while providing a simple and universal strategy for rapid and sensitive detection of mycotoxins in foodstuffs.

Keywords Aptasensor · Dual-readout · Aflatoxin B1 · FRET · Gold nanoparticles · Quantum dots

Introduction

Aflatoxin is a kind of metabolite produced by *Aspergillus flavus* and *Aspergillus parasiticus* in a hot and humid environment [1]. Currently, aflatoxins have been isolated and identified in more than 20 subtypes, among which aflatoxin B1 (AFB1) is the most toxic mycotoxin and is widely distributed in various agricultural products [2]. The International Agency for Research on Cancer has classified AFB1 as a class I carcinogen due to its strong carcinogenicity, teratogenicity, and mutagenicity [3]. Considering the serious health risks that may be generated by consuming foods contaminated with a high level of AFB1, many countries and organizations have established strict limits for AFB1 in agricultural products and proceed foods. For example, the U.S. Food and Drug Administration (FDA) requires that the maximum contamination level of AFB1 in all foods should not exceed 20 μg/kg [4]. To better reduce the risk of consumers' ingestion of AFB1-contaminated foods, it is urgently needed to develop a new method with advantages of rapidity, simplicity, sensitivity, and selectivity for monitoring AFB1 in agricultural products.

The currently developed AFB1 assays are mainly focused on instrumental assays and immunoassays. The instrumental analysis methods are sensitive, accurate, and reproducible, but usually suffered from the drawbacks of requiring sophisticated instruments, specialized operators, and complicated sample pretreatment [5]. Immunoassays based on high-affinity antigens and antibodies provide an alternative tool for AFB1

✉ Haiyang Jiang
haiyang@cau.edu.cn

[1] National Key Laboratory of Veterinary Public Health Security, College of Veterinary Medicine, China Agricultural University, Beijing 100193, China

[2] Beijing Key Laboratory of Detection Technology for Animal-Derived Food Safety, China Agricultural University, Beijing 100193, China

detection [6]. As the core reagents of immunoassays, antibodies have high production costs and are susceptible to interference by complex conditions, which have somewhat limited their application scenarios. The development of biosensors based on novel bio-recognition elements is of great interest to supplement the current limited analytical tools. The aptamer is an oligonucleotide sequence obtained by in vitro screening with various advantages such as high affinity, high specificity, low production cost, easy modification, and good stability [7]. To date, various aptasensors have been developed for detection of AFB1 based on colorimetric [8, 9], fluorometric [10], electrochemical [11], and surface-enhanced Raman scattering [12]. Most aptasensors require aptamer to be labeled on the probes, which will make the operations more sophisticated and affect the affinity of the aptamer bind to AFB1, thus reducing the sensitivity of the corresponding assays. Among them, colorimetric aptasensors have attracted widespread attention due to their easy operation, low cost, and friendly visual discrimination [13]. Gold nanoparticles (AuNPs) are the most commonly used signal tag in colorimetric aptasensors due to their superior optical characteristics, which allows us to easily modulate their dispersion and aggregation state to detect their color change [14]. However, colorimetric aptasensor usually suffer from limited sensitivity, the single signal output lacks self-calibration capability and is susceptible to interference from changes in operating conditions and biological environment.

Dual-mode sensing technology can effectively compensate for the inherent limitations of each sensing mode and integrate their unique advantages, thus significantly improving detection linear range, accuracy, and application flexibility, and showing some synergistic effect on the performance improvement of analytical methods [15]. Therefore, converting color signal into fluorescence signal to establish a sensitive dual-readout aptasensor for colorimetric/fluorometric detection of AFB1 is an ideal strategy. Fluorescence energy resonance transfer (FRET) is a non-radioactive energy transfer model that transfers nonradiative energy from fluorescent donor in close proximity to an acceptor via dipole-dipole interactions [16]. Generally, FRET requires the absorption of the acceptor to overlap with emission of fluorescent donors and satisfy the specific distance between donor and acceptor (typically lower than 10 nm)[17]. The specific distance requirement usually relies on covalent linkage utilizing protein interaction, antigen-antibody recognition, and DNA hybridizations to bring the distance closer [18, 19]. Cumbersome modification or labeling processes will inevitably complicate the operations while reducing the stability of the aptasensor. Electrostatic force–mediated non-covalent linkage is an ideal alternative compared to covalent linkage to generate FRET; it is a simpler and more efficient way to just select suitable donor/acceptor pairs to achieve FRET. Therefore, it is extremely important to select the appropriate donor/receptor pairs. Quantum dots (QDs) have aroused widespread interest in the field of sensing due to their advantages of tunable spectra, excellent photostability, high quantum yield, good water solubility, and large Stokes shift [20]. Moreover, their surface change can be easily tailored by changing the capping layer, thus providing favorable conditions for the construction of FRET sensing systems with donor/acceptor pairs using QDs and AuNPs, respectively. Our motivation in this work is to use an electrostatic force–mediated FRET strategy for smart signal conversion to develop a dual-mode aptasensor for AFB1 detection, which will bring more opportunities to apply the strategy to extend application analysis scenarios.

Herein, we developed a modification-free aptasensor for colorimetric/fluorometric dual-readout detection of AFB1 in food samples by using AuNPs and QDs as color and fluorescence signal labels, respectively (Scheme 1). In the presence of the AFB1, the AFB1 can specifically bind to the aptamer to form AFB1/AFB1 aptamer complex and desorb from the AuNPs, and the AuNP solution changed from wine-red to purple under the induced aggregation effect of NaCl accompanied by an absorbance decrease, which was inversely proportional to AFB1 concentration. Meanwhile, the positively charged QDs were introduced into reaction system to interact with negatively charged AuNPs to produce fluorescence quenching, which successfully converted the color signal into a more sensitive fluorescence signal via electrostatic force-mediated FRET. The fluorescence quenching efficiency decreased with increasing concentrations of AFB1 and the fluorescence of aptasensor gradually recovered; the AFB1 concentration was positively proportional to the variation of fluorescence intensity. Moreover, the proposed dual-readout aptasensor was successfully applied in detecting corn and wheat samples. The dual-readout modification-free aptasensor designed in this work has a variety of advantages such as modification-free, dual-readout, self-calibration, simple operation, and cost-effectiveness, which provided a promising strategy for simple and accurate detection of other mycotoxins in foodstuffs.

Materials and methods

Materials and reagents

$HAuCl_4 \cdot 3H_2O$, chitosan (CS), trisodium citrate (TSC), and (hydroxymethyl) methyl aminomethane (Tris) were purchased from Sigma-Aldrich Company (St. Louis, MO, USA). Sodium chloride (NaCl), magnesium chloride ($MgCl_2$), potassium chloride (KCl), calcium chloride ($CaCl_2$), sodium hydroxide (NaOH), and other reagents used in this study were all of analytical grade and provided by Sinopharm Chemical Reagent Beijing Co., Ltd. (Beijing, China). The amino and carboxylated modified CdSe/ZnS QDs (5 mg/mL) were purchased from Xingzi new material technology development Co., Ltd. (Shanghai, China). The commercial AFB1 ELISA kits were purchased from Beijing WDWK Biotechnology Co., Ltd. (Beijing, China). The

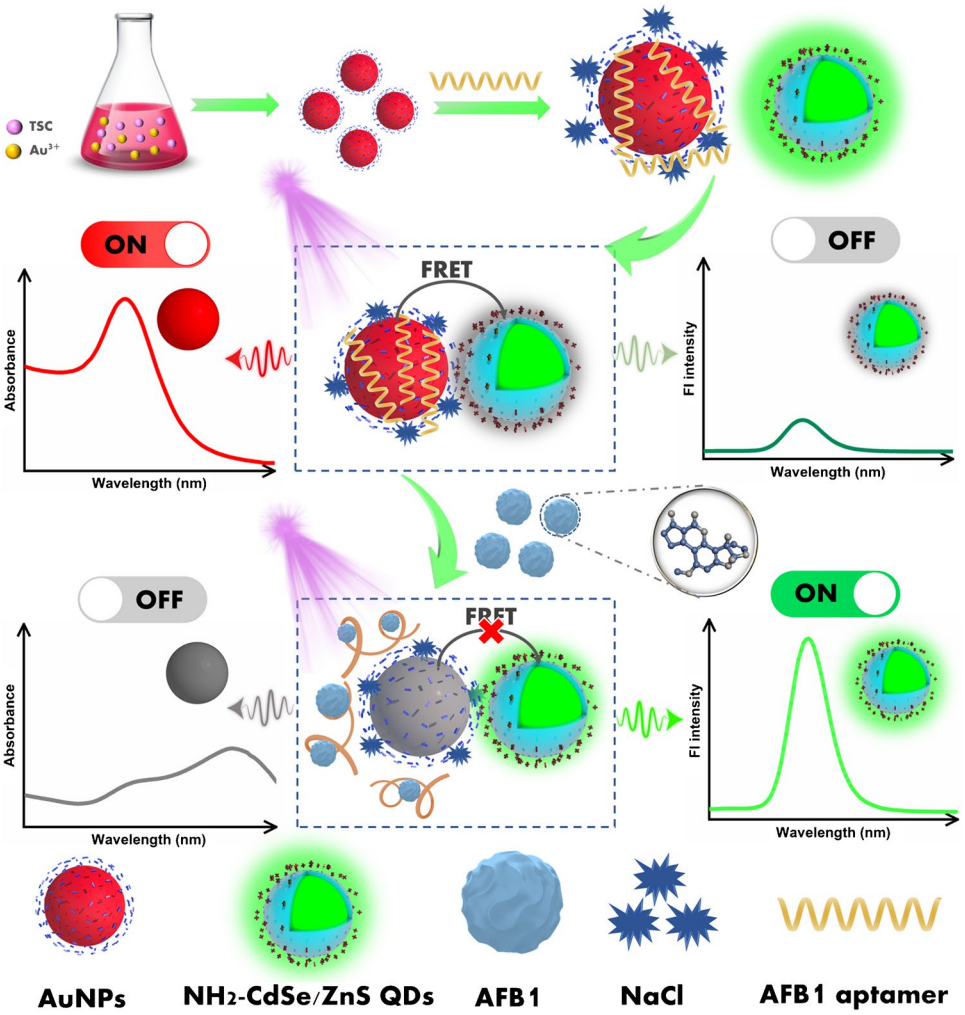

Scheme 1 Schematic illustration of the modification-free aptasensor for colorimetric/fluorometric dual-readout detection of AFB1 in foodstuffs (corn and wheat)

analyte standards (purity 99.0%) of aflatoxin B1 (AFB1), B2 (AFB2), M2 (AFG1), (AFG1), G2 (AFG2), ochratoxin A (OTA), Zearalenone (ZEN), and T-2 toxin (T-2) were purchased from the National Institutes for Food and Drug Control (Beijing, China). The AFB1 aptamer (5′-GTT GGG CAC GTG TT G TCT CTC TGT GTC TCG TGC CCT TCG CTA GGC CCA CA-3) was synthesized by Sangon Biotech (Shanghai, China) [10]. The corn and wheat samples were purchased from a local supermarket in Beijing. The working buffer used in this work is 10 mM Tris (pH=7.6, containing 50 mM Na^+, 2 mM Mg^{2+}, 5 mM K^+, 1 mM Ca^{2+})

Apparatus and characterization

The apparatus and characterization in detail are provided in the Supplementary Materials.

Synthesis of AuNPs and CS-AuNPs

The wine red-colored AuNPs were synthesized by the TSC reduction method according to the previously reported literature with slight modification [21]. The CS-AuNPs were prepared in accordance with our previous report [22]. The detailed synthesis process could be found in the Supplementary Materials.

Optimization of experimental conditions

In this work, five experimental parameters including NaCl concentration and its reaction time, aptamer concentration and its reaction time, incubation time, incubation temperature, and concentrations of QDs were investigated and specific optimization processes in detail are provided in the Supplementary Materials.

Procedure of FRET-based aptasensor for AFB1 detection

The detection procedure in detail is described as follows: the aptamer solution was heated at 95°C for 5 min and then left at room temperature for 30 min to form a stable spatial

conformation. A total of 20 μL of AFB1 standard solution or extract solution was mixed with 20 μL of 0.5 μM AFB1 aptamer at 25°C for 35 min. Afterward, 140 μL of AuNPs was added to the mixture and incubated for 8 min at 25°C, followed by the addition of 20 μL, 0.2 M NaCl solution, and incubated for 10 min at 25°C. After the reaction was completed, the resultant solution was transferred to a 96-well microplate and measured A_{650}/A_{520} ratio by a multifunctional reader. For fluorometric detection, 20 μL of 0.2 mg·mL^{-1} of QDs solution was added to completed colorimetric reaction system, the fluorescence intensity of 525-nm emission at the maximum excitation wavelength of 350 nm was measured, and fluorescence ratio (F-F0)/F0 was calculated.

Application of AFB1 detection in real samples

The corn and wheat samples were purchased from a local supermarket in Beijing and were confirmed as negative samples by National Reference Laboratory for Veterinary Drug Residues (Beijing, China) using UPLC-MS/MS. The confirmed negative samples were used for spiking analysis and methods validation to verify the practicability and reliability of the proposed aptasensor. Generally, several 1-g fine-grained samples were weighed and added AFB1 standard solution with four levels; the spiked samples experienced natural air-drying. Subsequently, 5 mL of methanol/water (7:3, v/v) solution was added and vortexed for 15 min at room temperature, followed by centrifugation at 4000 rpm for 10 min; the supernatant was filtered via a 0.22-μm membrane to remove impurities. The resultant solution was then diluted 5-fold with buffer for methods determination. Eventually, the results of proposed aptasensor were validated using commercial ELISA kits. Each sample was repeated at least three times.

Results and discussion

The testing principle of FRET-based dual-readout aptasensor

In this work, we designed a modification-free aptasensor for dual-readout detection of AFB1 via electrostatic force–mediated FRET using AuNPs and positively charged CdSe/ZnS QDs as color and fluorescence signal tags, respectively (Scheme 1). The dispersion and aggregation state variation of AuNPs was manifested by the change of solution color from wine-red to purple. The NaCl addition reduced the repulsive force between AuNPs and induced their aggregation. The bases of aptamer could easily be adsorbed on the surface of AuNPs through attractive forces, hydrophobic interactions, and van der Waals forces [23]. The electrostatic repulsion between aptamer and negatively charged AuNPs protected AuNPs from salt-induced aggregation, thus improving stability and maintaining the color wine-red of AuNPs. In the presence of AFB1, AFB1 aptamer underwent a conformational transition upon binding to AFB1, resulting in the formation of AFB1/AFB1 aptamer complex, thus leading the aptamer to release from the surface of AuNPs. The color of AuNP solution changed from wine-red to purple under the effect of NaCl-induced aggregation, and the absorbance value at 520 nm gradually decreased. The AFB1 concentration was inversely proportional to A_{520} absorbance value of AuNPs. Subsequently, we introduced an extra fluorescent label to further enhance sensitivity; the AuNPs displayed favorable spectral overlap with the emission of QDs, while the negatively charged AuNPs interacted with positively charged QDs via electrostatic attraction to bring them to a proper distance, and the color signal was successfully converted into fluorescent signal through FRET. The extent of spectral overlap between AuNPs and QDs gradually decreased with the increasing AFB1 concentration, thereby fluorescence signal gradually turned on, and the AFB1 concentration was directly proportional to the fluorescence intensity changes.

Feasibility analysis of dual-readout aptasensor

The TSC-stabilized AuNPs and NH_2-CdSe/ZnS QDs were characterized by transmission electron microscopy (TEM), UV-Vis and fluorescence spectrometry, and dynamic light scattering. The results in Fig. S1 demonstrated their good morphology and could be used as color and fluorescence tags for construction of dual-readout aptasensor, respectively.

Multiple methods including UV-Vis spectrum, zeta-potentials, and TEM are used for feasibility analysis of colorimetric aptasensor. As depicted in Fig. 1a, b), AuNPs solution presented color wine red with a zeta potential of −37.6 mV (Fig. 1a, inset a). After the NaCl-induced aggregation effect, the maximal absorption peak shifted from 520 to 650 nm and was accompanied by a change in color from wine red to purple (Fig. 1a, inset d), while the zeta potential increased to −26.4 mV. The aptamer-protected AuNPs remained color wine red after NaCl addition (Fig. 1a, inset b), the absorption peak did not change, and zeta potential decreased to −35.1 mV. In the presence of AFB1, AFB1 could specifically bind to form AFB1/AFB1 aptamer complex and desorbed from the surface of AuNPs, the aptamer lost its protective effect, and AuNPs underwent aggregation (Fig. 1a, inset c); the zeta potential also increased to −29.5 mV.

Furthermore, the TEM was employed to demonstrate the dispersion and aggregation state of AuNPs. The individual AuNPs exhibited spherical morphology with good distributions (Fig. 1c), while AuNPs underwent significant

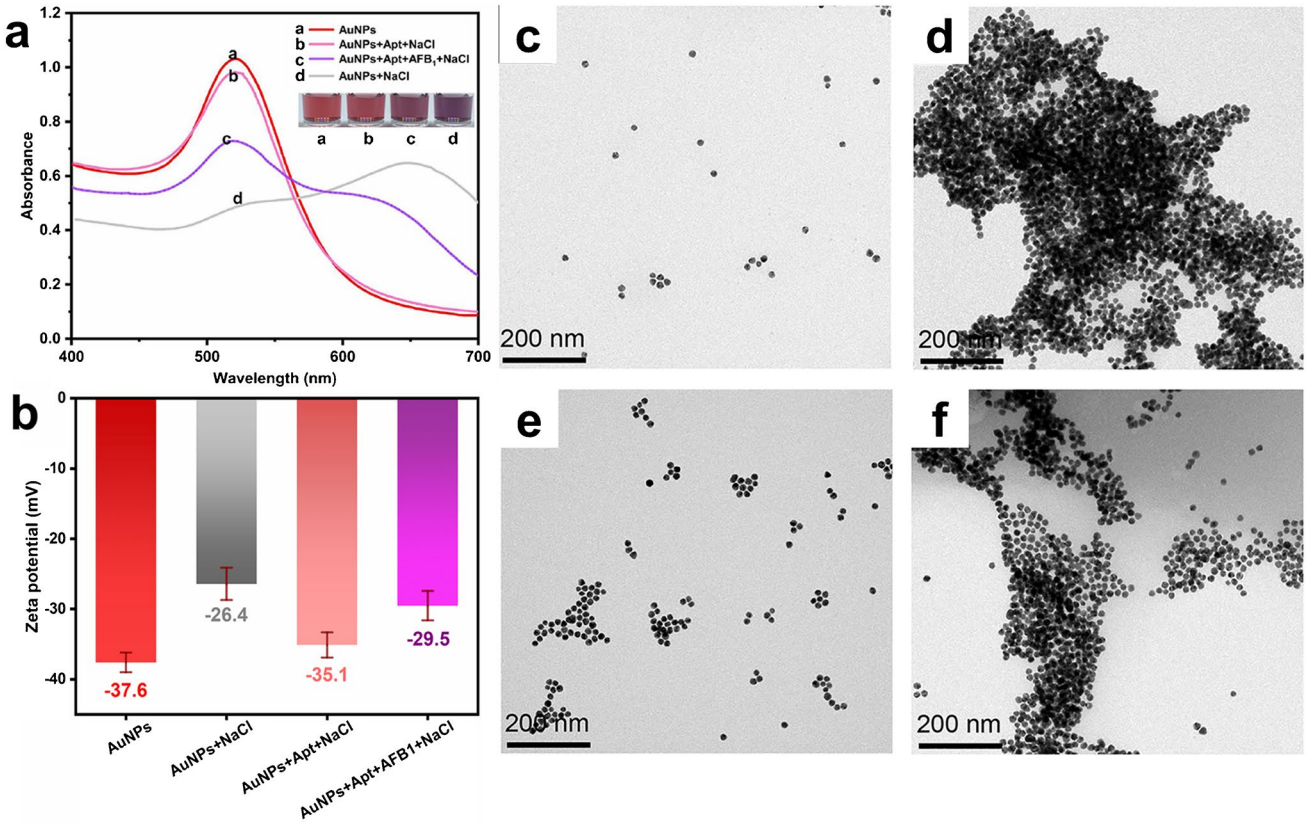

Fig. 1 The verification of the feasibility of colorimetric method. (**a**) UV-Vis spectrum of AuNPs under various conditions. Inset image: photograph of AuNPs changes within different states. (**b**) Zeta-potential variations of AuNPs treated with different substances. TEM images AuNPs (**c**), AuNPs + NaCl (**d**), AuNPs + Aptamer + NaCl (**e**), AuNPs+ Aptamer + NaCl +AFB1 (**f**)

aggregation with the addition of NaCl (Fig. 1d). Subsequently, the aptamer was introduced into AuNP solution and absorbed on the surface of AuNPs, the aptamer-protected AuNPs from NaCl-induced aggregation maintained a well-dispersed state (Fig. 1e). The addition of AFB1 into aptamer-protected AuNPs resulted in re-aggregation of AuNPs (Fig. 1f). These results demonstrated that the aptamer could adsorb on the surface of AuNPs and protect them from NaCl-induced electrostatic shielding, the AFB1 specifically bound to aptamer to form AFB1/aptamer complex and desorbed from the surface of AuNPs, losing their stability in the salt solution and transformed from the dispersed to the aggregated state, thereby obtaining visually apparent color changes and quantifiable absorbance value changes.

To further improve the sensitivity of aptasensor, it is an ideal strategy to introduce fluorescence signal to achieve signal amplification for detecting trace levels of AFB1 in foodstuffs. The common fluorescence sensing mechanism mainly involves FRET and inner filter effect (IFE) [22]. IFE is a simple approach that only requires the spectral overlap between donor and acceptor to occur, but their fluorescence quenching efficiency is low and susceptible to non-specific quenching due to interference from external environment [24]. In contrast, the FRET needs to satisfy a specific distance between donor and acceptor to realize electron or energy transfer process, which ensures specificity of analysis process and reduces interference [25]. Therefore, choosing a simple and convenient strategy to develop a highly specific and sensitive FRET-based aptasensor is attractive. As shown in Fig. 2a, the absorption peak of AuNPs and excitation peak of QDs were located at 520 and 525 nm, respectively, which achieved a perfect overlap between acceptor and donor. Then the fluorescence spectrum of QDs under different reaction conditions was determined and as depicted in Fig. 2b. The dispersed AuNPs could significantly quench the fluorescence of QDs (Fig. 2b, inset d), the extent of spectral overlap between salt-induced aggregated AuNPs and QDs decreased, leading to fluorescence recovery (Fig. 2b, inset a), the aptamer-protected AuNPs remained dispersed and quenched the fluorescence of QDs (Fig. 2b, inset c), the addition of AFB1 made the aptamer no longer able to protect the AuNPs, and the AuNPs underwent aggregated and fluorescence restored to some extent. In addition, other substances in the reaction system did not interfere with fluorescence intensity of QDs except AuNPs, indicating the good anti-interference capability of

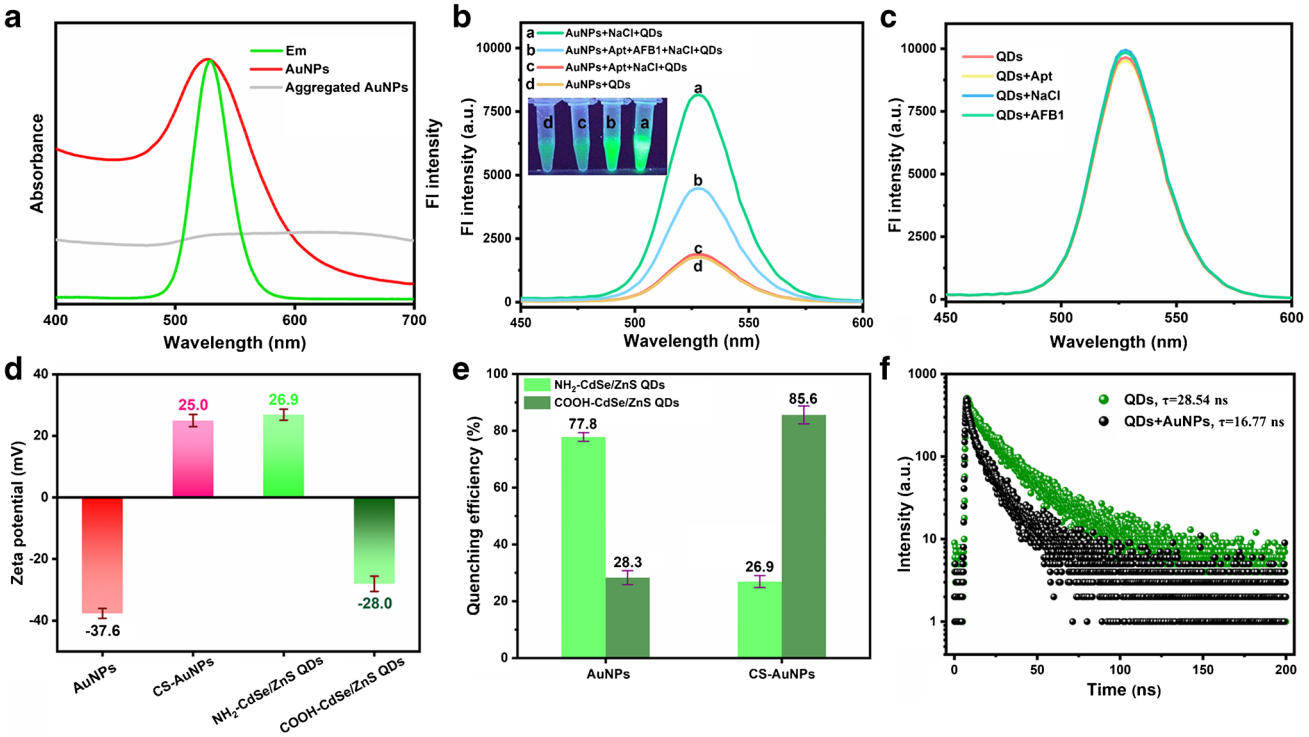

Fig. 2 The validation of the feasibility of fluorometric method and FRET mechanism. (**a**) Spectral overlap between AuNPs and QDs. (**b**) Fluorescence spectrum of QDs under various conditions. Inset image: photograph of QDs changes with a different state. (**c**) The fluorescence spectrum of QDs co-exists with other substances. (**d**) Zeta-potentials of AuNPs, CS-AuNPs, NH_2-CdSe/ZnS QDs, and COOH-CdSe/ZnS QDs. (**e**) Comparison of fluorescence quenching efficiency of AuNPs/QDs pairs. (**f**) Fluorescence lifetime decay of QDs, and mixture of AuNPs and QDs

QDs in reaction system (Fig. 2c). Moreover, we determined the linear relationship between different AuNP concentrations and the fluorescence quenching ratio of QDs. As illustrated in Fig. S2, the concentration of AuNPs showed a good linear relationship with the fluorescence quenching ratio in the range of 0–2 nM, and the Stern-Volmer equation was presented as $I0/I=2.7385C(\text{AuNPs})\times[Q]+1$ ($R^2=0.994$). These results indicated that we could easily regulate the change of fluorescence intensity of QDs by adjusting the aggregation and dispersion state of AuNPs to achieve the conversion from color signal into fluorescence signal, thereby improving the detection sensitivity.

To better understand difference in quenching efficiency between FRET and IFE, more characterizations were performed. As shown in Fig. 2d, the zeta-potentials of AuNPs, CS-AuNPs, NH_2-QDs, and COOH-QDs were −37.6, 25.0, 26.9, and −28.0 mV, respectively. The NH_2-QDs/AuNPs and COOH-QDs/CS-AuNPs donor/acceptor pairs would generate highly efficient FRET due to excellent electrostatic attraction; the donor/acceptor pair with the same charge would produce IFE. As noted in Fig. 2e, the quenching efficiency of NH_2-QDs/AuNPs was 2.75 times higher than COOH-QDs/AuNPs, and the quenching efficiency of COOH-QDs/CS-AuNPs was 3.18 times higher than NH_2-QDs/CS-AuNPs. The donor and acceptor can generate strong interactions to facilitate the transfer of electron energy from the donor to the acceptor due to electrostatic force–mediated FRET; IFE does not produce this electron energy transfer due to their charge repulsion between donor and acceptor, so their quenching efficiency is significantly lower than FRET [26]. The adoption of suitable donor/acceptor pairs to produce electrostatic-force FRET for sensing is beneficial to maximizing quenching efficiency and improving corresponding detection sensitivity.

We further investigated the sensing mechanism by determining the fluorescence lifetime decay of QDs and mixture of AuNP with QDs. FRET is a non-radiative energy transfer process where the energy generated by the donor in the excited state is transferred to the acceptor, which leads to both fluorescence quenching and lifetime shortening of the donor [17]. IFE results in quenching of the emission of fluorescent donors but does not involve a change in fluorescence lifetime [22]. The fluorescence lifetime of QDs alone and in the presence of AuNPs was 28.54 ns and 16.77 ns, respectively (Fig. 2f), and this result excluded that the fluorescence quenching was caused by IFE. Therefore, the quenching mechanism by AuNPs toward NH_2-QDs could be ascribed to FRET.

Optimization of assay conditions

Systematic optimization of assay conditions optimization is essential to obtain optimal detection performances of developed aptasensor. The optimal assay conditions were chosen as the NaCl concentration (0.2 M) and its reaction time (10 min), aptamer concentration (0.2 μM) and its reaction time (8 min), incubation time (35 min), incubation temperature (25°C), and concentrations of QDs (0.2 mg·mL^{-1}), shown in Supplementary Materials.

Sensitivity and selectivity of dual-readout aptasensor for AFB1 detection

With optimized experimental conditions, the sensitivity of proposed dual-readout aptasensor was evaluated. A series of different concentrations of AFB1 was added to the mixture of AuNPs/AFB1 aptamer/NaCl. As illustrated in Fig. 3a, the absorbance value at 520 nm gradually decreased as the concentration of AFB1 increased. This result indicated that specific interaction occurred between aptamer and AFB1 and more aptamer/AFB1 complex formation made aptamer release from the surface of AuNPs, the AuNPs aggregated under the addition of NaCl, resulting in decreasing absorbance. The inset of Fig. 3a shows the color of AuNPs varies with the increasing concentration of AFB1 under natural light. The color of AuNP solution gradually changed from wine-red to purple with the concentration of AFB1 from low to high, which meant we could easily distinguish the appropriate concentration of AFB1 by color signal for semi-quantitative analysis. Subsequently, the linear relationship of A_{650}/A_{520} versus AFB1 concentration was determined and is presented in Fig. 3b. The colorimetric aptasensor had good linearity in the range of 10–320 ng·mL^{-1}, and the calibration equation was presented as y=0.0039x + 0.0746 with a correlation coefficient (R^2) of 0.993. The limit of detection (LOD) was defined as the mean of A_{650}/A_{520} value of AFB1 free buffer solution plus three times standard deviation and calculated to be 7.32 ng·mL^{-1}. The sensitivity of colorimetric aptasensor provided herein met the regulatory requirements of the FDA for AFB1 in foodstuffs.

To further improve the sensitivity of proposed aptasensor, the positively charged green-emitting QDs were introduced into sensing system to interact with negatively charged AuNPs and generate FRET via electrostatic force, thus realizing the conversion from color signal to fluorescence signal. As depicted in Fig. 3c, the fluorescence intensity gradually turned on as the concentration of AFB1 increased. The AuNPs from dispersion to aggregation state were accompanied by a decrease in the area of spectral-overlap between AuNPs with QDs, thereby reducing FRET efficiency and fluorescence turned on. The inset of Fig. 3c clearly shows the fluorescence signal gradually turned on with increasing AFB1 concentration under a UV lamp. The linear

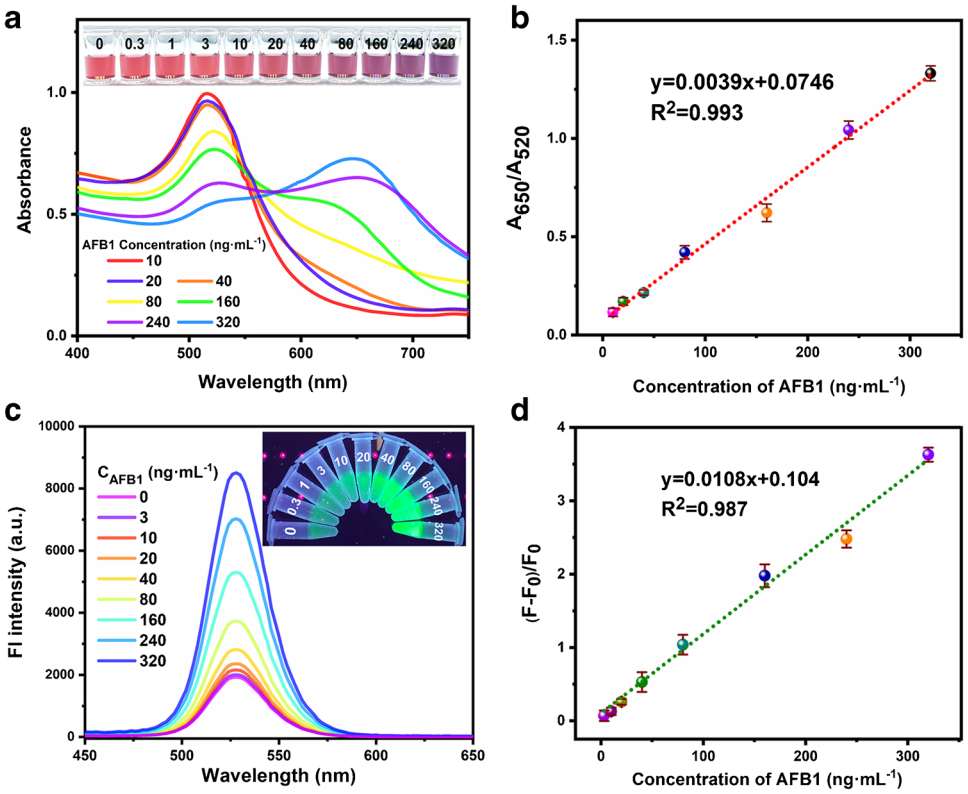

Fig. 3 The sensitivity of dual-readout aptasensor for AFB1 detection. **a** UV-Vis absorption spectrum of AuNPs in the presence of different amounts of AFB1. The inset image showed visual color changes of colorimetric aptasensor with various concentrations under natural light. **b** The linear relationship of A_{650}/A_{520} value of AuNPs versus AFB1 concentration. **c** Fluorescence spectrum of QDs in the presence of different amounts of AFB1. The inset image showed fluorescence changes of fluorometric aptasensor with various concentrations under UV light. The fluorescence intensity of 525-nm emission at the maximum excitation wavelength of 350 nm was measured. **d** The linear relationship of (F-F0)/F0 value of QDs versus AFB1 concentration

relationship between (F-F0)/F0 and AFB1 concentration is presented in Fig. 3d. The fluorometric aptasensor provided a wide linear range from 3 to 320 ng·mL^{-1}. The linear regression equation was y=0.0108x + 0.104 with R^2=0.987, and LOD was calculated to 1.48 ng·mL^{-1} (the mean of (F-F0)/F0 value of AFB1 free buffer solution plus three times standard deviation), which was approximately 5-fold higher than colorimetric aptasensor. The fluorometric aptasensor provides a wider linear range and higher detection sensitivity, which is suitable for effectively monitoring AFB1 at trace levels in food samples.

The selectivity of proposed dual-readout aptasensor was evaluated by selecting other seven mycotoxins including AFB2, AFM2, AFG1, AFG2, OTA, ZEN, and T2 as interfering substances. The AFB1 and the other seven mycotoxins were 200 and 500 ng·mL^{-1}, respectively. Figure 4a reveals that only AFB1 could interact with AFB1 specific aptamer for the formation of aptamer/AFB1 complex and released from the surface of AuNPs, inducing AuNPs aggregate accompanied by an obvious improvement of A_{650}/A_{520} value. The value of A_{650}/A_{520} remained unchanged with the addition of the other seven mycotoxins, indicating that there were no interactions between interfering substances and AFB1 aptamer. Meanwhile, the obvious fluorescence intensity variation was observed with the addition of AFB1, and no significant changes were observed for the other seven mycotoxins (Fig. 4b). The established dual-readout aptasensor has favorable selectivity for AFB1 detection.

The recently published aptasensors for AFB1 detection were selected for comparison of detection performances from several indicators (e.g., signal types, signal tags, recognition probe, linear range, LOD, and samples) with our developed dual-readout aptasensor. As shown in Table 1, the developed dual-readout aptasensor in this work has obvious novelty and advantages. A simple mixture of AuNPs, aptamer, NaCl, and QDs allows rapid dual-readout determination of AFB1 without additional labeling and modification of the signal tags, simplifying operations and enhancing efficiency, which provides considerable convenience for on-site detection. The colorimetric and fluorometric detection is

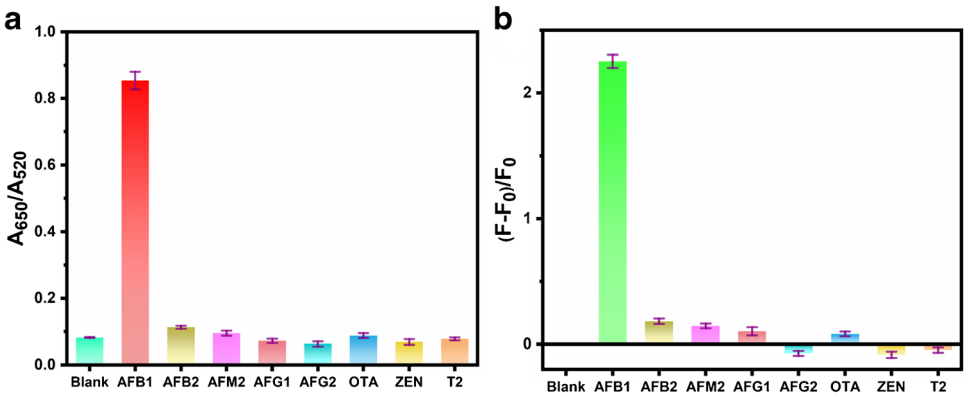

Fig. 4 The selectivity of dual-readout aptasensor. **a** Colorimetric method. **b** Fluorometric method. The AFB1 and other toxins were 200 and 500 ng·mL^{-1}, respectively

Table 1 Comparison of detection performances of recently developed aptasensors for AFB1 detection

Signal	Signal tags	Recognition probe	Linear range (ng·mL^{-1} or ng·g^{-1})	LOD (ng·mL^{-1} or ng·g^{-1})	Samples	Reference
Color	AuNPs	Modification-free	0.36	1–10	Rice/peanut	[8]
Color	PS NPs	Single-labeled	5–1000	4.56	Peanut/corn/rice/chili powder	[9]
Fluorescence	FAM	Dual-labeled	5–100	1.6	Rice cereal	[27]
Fluorescence	Cy5	Dual-labeled	0.3–10	0.1	Corn	[28]
Fluorescence	AIE	Modification-free	40–300	27.3	Broad bean paste/peanut oil	[29]
CL	HRP-DNAzyme	Dual-labeled	0.1–10	0.11	Corn	[30]
ECL	PtFe@Co-MOF	Dual-labeled	0.005–80	0.002	Corn	[11]
SERS	Ag@Au NPs	Dual-labeled	0.03–100	0.03	Maize meal	[12]
Color/fluorescence	AuNPs/NH_2-CdSe/ZnS QDs	Modification-free	10–400/ 3–400	7.32/1.48	Corn/wheat	This work

PS NPs, polystyrene dyed particles; *FAM* and *CY5*, fluorescein; *AIE*, aggregated-induced emission; *PtFe@Co-MOF*, Pt Fe doped NH_2-Co-MOF; *Ag@Au NPs*, Ag@Au core–shell nanoparticles

Table 2 Accuracy and precision of fluorescent aptasensor for quantitative detection of AFB1 in spiked corn and wheat samples

Samples	Spiked concentration ($\mu g \cdot kg^{-1}$)	Intra-assay (n=3)		Inter-assay (n=9)	
		Recovery (%)	RSD (%)	Recovery (%)	RSD (%)
Corn	10	93.2	5.6	91.3	6.9
	50	92.8	8.3	102.9	12.6
	100	89.3	7.4	85.3	13.2
	200	102.3	6.3	110.4	9.5
Wheat	10	91.8	6.4	88.3	10.1
	50	93.8	4.9	105.6	7.8
	100	103.6	8.2	106.9	12.4
	200	104.7	5.5	113.4	13.3

RSD relative standard deviation

integrated into one platform facilitating self-calibration and effectively improving the analysis accuracy of the aptasensor, differentiated detection linear range, and sensitivity which could satisfy detection requirements for AFB1 at various regions, greatly improving the application flexibility in practical applications. The color signal under natural light and fluorescence signal under UV light are simultaneously provided, and friendly visual discrimination can meet the qualitative and semi-quantitative demands of AFB1 detection in different application scenarios. The AuNPs and QDs are the most commonly used signal tags for constructing colorimetric/fluorometric sensors due to their facile synthesis, superior stability, and low cost, which will provide a more cost-effective detection tool for resource-poor regions. More importantly, electrostatic force-mediated FRET is a simple and convenient strategy that produces high fluorescence quenching efficiency and low background fluorescence signal and possesses good anti-interference capability, increasing the detection sensitivity of aptasensor to a satisfactory level. Although the proposed aptasensor has no significant advantage compared to other methods in terms of sensitivity, it can still meet the requirements of different countries for AFB1 detection in grain, while we make significant improvements in terms of simplicity, cost, functionality, and practicality.

Application in corn and wheat samples

To verify the applicability of proposed fluorescent aptasensor in actual samples, the recovery of AFB1 spiked corn and wheat samples at four different levels (10, 50, 100, and 200 $\mu g \cdot kg^{-1}$) were determined. The spiked procedures were used to simulate the true state of contaminated samples as closely as possible. The results are shown in Table 2; the average recoveries of intra-day ranged from 89.3 to 104.7% with RSD values less than 8.3%. The average recoveries of inter-day ranged from 85.3 to 113.4% with RSD value in the range of 6.9–13.3%. These results demonstrated the established fluorescent aptasensor in corn and wheat samples had good accuracy and precision. Moreover, four different levels of AFB1 spiked corn and wheat samples were simultaneously determined by fluorescent aptasensor and commercial ELISA kits with three replicates per sample. As noted in Fig. S5, the detection results of fluorescent aptasensor agreed with commercial ELISA kits with an R^2=0.998. These results demonstrated that the proposed fluorescent aptasensor could be applied for detection of actual food samples (corn and wheat).

Conclusions

In summary, we developed a novel modification-free aptasensor for colorimetric/fluorometric dual-readout detection of AFB1 in foodstuffs. Based on the interactions between AFB1, AFB1 specific aptamer, and AuNPs, the color variations of AuNPs could be easily observed visually and measured absorbance values for colorimetric quantitative analysis in the presence of AFB1. Moreover, the positively charged QDs were introduced into reaction system and interacted with AuNPs, which successfully converted the color signal into a more sensitive fluorescence signal via electrostatic force-mediated FRET. The LOD of fluorometric aptasensor achieved an approximately 5-fold improvement compared to the colorimetric aptasensor. The accuracy, precision, and reliability of dual-readout aptasensor were further validated by spiking experiments and methods comparison. The proposed aptasensor herein integrates multiple advantages such as modification-free, dual-readout, self-calibration, easy operation, and cost-effectiveness, which provides a powerful on-site tool for the sensitive and selective detection of AFB1 in food samples. Despite the satisfactory analytical performance, how to choose a suitable signal amplification strategy to further improve the sensitivity to achieve monitoring of the trace level of AFB1 is still a challenging problem. In addition, the existing electrostatic-force mediated donor/acceptor pairs are scarce; there is a need to further seek high-performance donor/receptor pairs in the future and explore their application in FRET analysis.

Supplementary Information The online version contains supplementary material available at https://doi.org/10.1007/s00604-023-05641-1.

Author contributions Jincheng Xiong: conceptualization, data curation, formal analysis, writing—original draft. Shuang He: investigation, methodology, data analysis. Linqian Qin: investigation, methodology. Shuai Zhang: methodology, data curation. Wenchong Shan: investigation, data curation, formal analysis. Haiyang Jiang: resources; supervision; writing—review and editing; funding acquisition; project administration.

Funding We gratefully acknowledge the support of Beijing Natural Science Foundation of China (Grant No. 6222021).

Declarations

Conflict of interest The authors declare no competing interests.

References

1. Goud KY, Kailasa SK, Kumar V, Tsang YF, Lee SE, Gobi KV, Kim K-H (2018) Progress on nanostructured electrochemical sensors and their recognition elements for detection of mycotoxins: a review. Biosens Bioelectron 121:205–222. https://doi.org/10.1016/j.bios.2018.08.029
2. Xu N, Xiao Y, Xie Q, Li Y, Ye J, Ren D (2021) Occurrence of aflatoxin B1 in total mixed rations and aflatoxin M1 in raw and commercial dairy milk in northern China during winter season. Food Control 124:107916. https://doi.org/10.1016/j.foodcont.2021.107916
3. IARC (1993) IARC monographs on the evaluation of carcinogenic risks to humans: some naturally occurring substances: Food Items and Constituents. In: Heterocyclic Aromatic Amines and Mycotoxins, vol 56. international Agency for Research on Cancer, UK
4. U.S. Food and Drug Administration (FDA) (2021) Manual of compliance policy guides-694 chapter 5-food, colors, and cosmetics [EB/OL] [2021-06-29].
5. Maragos CM, Busman M (2010) Rapid and advanced tools for mycotoxin analysis: a review. Food Addit Contam Part A 27(5):688–700. https://doi.org/10.1080/19440040903515934
6. Matabaro E, Ishimwe N, Uwimbabazi E, Lee BH (2017) Current immunoassay methods for the rapid detection of aflatoxin in milk and dairy products. Compr Rev Food Sci Food Saf 16(5):808–820. https://doi.org/10.1111/1541-4337.12287
7. Chen A, Yang S (2015) Replacing antibodies with aptamers in lateral flow immunoassay. Biosens Bioelectron 71:230–242. https://doi.org/10.1016/j.bios.2015.04.041
8. Lerdsri J, Chananchana W, Upan J, Sridara T, Jakmunee J (2020) Label-free colorimetric aptasensor for rapid detection of aflatoxin B1 by utilizing cationic perylene probe and localized surface plasmon resonance of gold nanoparticles. Sens. Actuators B 320:128356. https://doi.org/10.1016/j.snb.2020.128356
9. Vijitvarasan P, Cheunkar S, Oaew S (2022) A point-of-use lateral flow aptasensor for naked-eye detection of aflatoxin B1. Food Control 134:108767. https://doi.org/10.1016/j.foodcont.2021.108767
10. Xiong J, He S, Zhang S, Qin L, Yang L, Wang Z, Zhang L, Shan W, Jiang H (2023) A label-free aptasensor for dual-mode detection of aflatoxin B1 based on inner filter effect using silver nanoparticles and arginine-modified gold nanoclusters. Food Control 144:109397. https://doi.org/10.1016/j.foodcont.2022.109397
11. Zhu T, Li N, Huang J, Xu X, Su X, Ma Y, Yang R, Ruan J, Su H (2022) An electrochemical aptasensor based on target triggered multiple-channel DNAzymes cycling amplification strategy with PtFe@Co-MOF as signal amplifier. Microchim Acta 189(10):388. https://doi.org/10.1007/s00604-022-05478-0
12. Zhao Y, Yang Y, Luo Y, Yang X, Li M, Song Q (2015) Double detection of mycotoxins based on SERS labels embedded Ag@Au core–shell nanoparticles. ACS Appl. Mater. Interfaces 7(39):21780–21786. https://doi.org/10.1021/acsami.5b07804
13. Hou Y, Jia B, Sheng P, Liao X, Shi L, Fang L, Zhou L, Kong W (2022) Aptasensors for mycotoxins in foods: recent advances and future trends. Compr Rev Food Sci Food Saf 21(2):2032–2073. https://doi.org/10.1111/1541-4337.12858
14. Quesada-González D, Stefani C, González I, de la Escosura-Muñiz A, Domingo N, Mutjé P, Merkoçi A (2019) Signal enhancement on gold nanoparticle-based lateral flow tests using cellulose nanofibers. Biosens Bioelectron 141:111407. https://doi.org/10.1016/j.bios.2019.111407
15. Zhou Y, Huang X, Hu X, Tong W, Leng Y, Xiong Y (2021) Recent advances in colorimetry/fluorimetry-based dual-modal sensing technologies. Biosens Bioelectron 190:113386. https://doi.org/10.1016/j.bios.2021.113386
16. Wu S, Duan N, Ma X, Xia Y, Wang H, Wang Z, Zhang Q (2012) Multiplexed fluorescence resonance energy transfer aptasensor between upconversion nanoparticles and graphene oxide for the simultaneous determination of mycotoxins. Anal Chem 84(14):6263–6270. https://doi.org/10.1021/ac301534w
17. Pehlivan ZS, Torabfam M, Kurt H, Ow-Yang C, Hildebrandt N, Yuce M (2019) Aptamer and nanomaterial based FRET biosensors: a review on recent advances (2014-2019). Microchim Acta 186(8):563. https://doi.org/10.1007/s00604-019-3659-3
18. Lu X, Wang C, Qian J, Ren C, An K, Wang K (2019) Target-driven switch-on fluorescence aptasensor for trace aflatoxin B1 determination based on highly fluorescent ternary CdZnTe quantum dots. Anal Chim Acta 1047:163–171. https://doi.org/10.1016/j.aca.2018.10.002
19. Xiang L, Tang J (2017) QD-aptamer as a donor for a FRET-based chemosensor and evaluation of affinity between acetamiprid and its aptamer. Rsc Advances 7(14):8332–8337. https://doi.org/10.1039/c6ra26118c
20. Hildebrandt N, Spillmann CM, Algar WR, Pons T, Stewart MH, Oh E, Susumu K, Diaz SA, Delehanty JB, Medintz IL (2017) Energy transfer with semiconductor quantum dot bioconjugates: a versatile platform for biosensing, energy harvesting, and other developing applications. Chem Rev 117(2):536–711. https://doi.org/10.1021/acs.chemrev.6b00030
21. Li JF, Tian XD, Li SB, Anema JR, Yang ZL, Ding Y, Wu YF, Zeng YM, Chen QZ, Ren B, Wang ZL, Tian ZQ (2013) Surface analysis using shell-isolated nanoparticle-enhanced Raman spectroscopy. Nat Protoc 8(1):52–65. https://doi.org/10.1038/nprot.2012.141
22. Xiong J, He S, Wang Z, Xu Y, Zhang L, Zhang H, Jiang H (2022) Dual-readout fluorescence quenching immunochromatographic test strips for highly sensitive simultaneous detection of chloramphenicol and amantadine based on gold nanoparticle-triggered photoluminescent nanoswitch control. J Hazard Mater 429:128316. https://doi.org/10.1016/j.jhazmat.2022.128316
23. Liu J (2012) Adsorption of DNA onto gold nanoparticles and graphene oxide: surface science and applications. Phys Chem Chem Phys 14(30):10485–10496. https://doi.org/10.1039/c2cp41186e
24. Chen S, Yu Y-L, Wang J-H (2018) Inner filter effect-based fluorescent sensing systems: a review. Anal Chim Acta 999:13–26. https://doi.org/10.1016/j.aca.2017.10.026
25. Singuru MMR, Sun SC, Chuang MC (2020) Advances in oligonucleotide-based detection coupled with fluorescence resonance

energy transfer. TrAC Trends Anal Chem 123:115756. https://doi.org/10.1016/j.trac.2019.115756
26. Goryacheva OA, Beloglazova NV, Goryacheva IY, De Saeger S (2021) Homogenous FRET-based fluorescent immunoassay for deoxynivalenol detection by controlling the distance of donor-acceptor couple. Talanta 225:121973. https://doi.org/10.1016/j.talanta.2020.121973
27. Chen L, Wen F, Li M, Guo X, Li S, Zheng N, Wang J (2017) A simple aptamer-based fluorescent assay for the detection of Aflatoxin B1 in infant rice cereal. Food Chem 215:377–382. https://doi.org/10.1016/j.foodchem.2016.07.148
28. Shim W-B, Kim MJ, Mun H, Kim M-G (2014) An aptamer-based dipstick assay for the rapid and simple detection of aflatoxin B1. Biosens Bioelectron 62:288–294. https://doi.org/10.1016/j.bios.2014.06.059
29. Xia X, Wang H, Yang H, Deng S, Deng R, Dong Y, He Q (2018) Dual-terminal stemmed aptamer beacon for label-free detection of aflatoxin B1 in broad bean paste and peanut oil via aggregation-induced emission. J Agric Food Chem 66(46):12431–12438. https://doi.org/10.1021/acs.jafc.8b05217
30. Shim W-B, Mun H, Joung H-A, Ofori JA, Chung D-H, Kim M-G (2014) Chemiluminescence competitive aptamer assay for the detection of aflatoxin B1 in corn samples. Food Control 36(1):30–35. https://doi.org/10.1016/j.foodcont.2013.07.042